Wright State University
CORE Scholar

Browse all Theses and Dissertations | Theses and Dissertations

2007

Detection and Destruction of *Escherichia Coli* Bacteria and Bacteriophage Using Biofunctionalized Nanoshells

Joseph E. Van Buren
Wright State University

Follow this and additional works at: https://corescholar.libraries.wright.edu/etd_all

 Part of the Molecular Biology Commons

Repository Citation

Van Buren, Joseph E., "Detection and Destruction of *Escherichia Coli* Bacteria and Bacteriophage Using Biofunctionalized Nanoshells" (2007). *Browse all Theses and Dissertations*. 190.
https://corescholar.libraries.wright.edu/etd_all/190

This Thesis is brought to you for free and open access by the Theses and Dissertations at CORE Scholar. It has been accepted for inclusion in Browse all Theses and Dissertations by an authorized administrator of CORE Scholar. For more information, please contact library-corescholar@wright.edu.

DETECTION AND DESTRUCTION OF *ESCHERICHIA COLI* BACTERIA AND BACTERIOPHAGE USING BIOFUNCTIONALIZED NANOSHELLS

A thesis submitted in partial fulfillment
of the requirements for the degree of
Master of Science

By

JOSEPH EDWARD VAN NOSTRAND
Ph.D., University of Illinois at Urbana/Champaign, 1996
M.S., Clarkson University, 1991
B.S., Clarkson University, 1988

2007
Wright State University

WRIGHT STATE UNIVERSITY

SCHOOL OF GRADUATE STUDIES

25 July 2007

I HEREBY RECOMMEND THAT THE THESIS PREPARED UNDER MY SUPERVISION BY Joseph Edward Van Nostrand ENTITLED Detection and Destruction of *Escherichia coli* Bacteria and Bacteriophage Using Biofunctionalized Nanoshells BE ACCEPTED IN PARTIAL FULFILLMENT OF THE REQUIREMENTS FOR THE DEGREE OF Master of Science.

_____

Madhavi P. Kadakia, Ph.D.
Thesis Director

_____

Daniel T. Organisciak, Ph.D.
Department Chair

Committee on
Final Examination

_____

Madhavi P. Kadakia, Ph.D.

_____

Rajesh R. Naik, Ph.D.

_____

John V. Paietta, Ph.D.

_____

Oleg Paliy, Ph.D.

_____

Joseph F. Thomas, Jr., Ph.D.
Dean, School of Graduate Studies

ABSTRACT

Van Nostrand, Joseph Edward. M.S., Department of Biochemistry and Molecular Biology, Wright State University, 2007. Detection and destruction of *Escherichia coli* bacteria and bacteriophage using biofunctionalized nanoshells

The ability to detect chemical and biological agents is arguably one of the highest priority technical challenges today. The capability to obtain specific information at and near single-molecule resolution is the ultimate goal in chemical and biological agent detection. Metallic nanostructures, nanoshells and nanorods in particular, are attractive substrates because of their plasmonic properties. Combining the specificity of biomolecular recognition with these nanostructures might lead to increased sensitivity and selectivity. Localization of biological recognition motifs to the surface of these nanostructures could provide a mechanism for highly specific and directed energy transfer when bound to its target. This study utilizes nanoshells functionalized with antibodies specific for *Escherichia coli*, and investigates at both the microscopic and macroscopic scales the ability of these biofunctionalized nanoshells to bind and destroy their target micro-organism when excited using 808 nm near infrared laser radiation. Extension of the technique to *Bacillus subtilis* spores as well as bacteriophage specific to *Escherichia coli* are also explored. The bacteriophage is a viral surrogate, and provides a means to explore proof of principle of the interactions between nanoshells and viruses. It is demonstrated that appropriately

biofunctionalized nanoshells recognize and bind to their target species, and that the nanoshell successfully couples the energy transfer from an IR laser to the target species. A ratio of nanoshells to *Escherichia coli* of ~10^4 for a 50% bacterial cell survival rate is determined, and a possible mechanism for this is discussed. Finally, this ratio is found to decrease by 4-5 orders of magnitude for the case of two *Escherichia coli* bacteriophage considered, and the significance of this is described.

TABLE OF CONTENTS

LIST OF FIGURES

LIST OF TABLES

DEDICATION

For Becky, Nicholas, Matthew, and Maria, whose support and patience I greatly appreciate.

I. INTRODUCTION

Techniques for detection of pathogenic microorganisms

The potential use of highly pathogenic microorganisms as biological weapons has spurred efforts to develop materials systems and techniques that have the capability to detect, quantify, and destroy these agents in a timely fashion (Atlas, 2001; Atlas, 2002; Bhalla, 2004; Bell, 2002). Many approaches have the ultimate goal of detecting levels as low as individual colony forming units of, for example, the spore forming bacterium Bacillus anthracis, where infection will lead to near certain mortality if medical treatment is not received within 24 hours of infection (Atlas, 2001). Several standard biochemical techniques are currently utilized for positive identification of microbial organisms. These include immunospecific assays, gene sequencing using polymerase chain reaction (PCR), and growth of colonies on nutrient rich plates followed by observation of colony morphology and response to various antibiotics, to name only a few. These research areas in biochemistry and molecular biology often employ methods that have proven to be extremely reliable, but require numerous biochemical protocols, appropriate laboratory facilities, and a highly technically competent staff. The

time required to obtain reliable results also suggests these methods are not amenable to real-time monitoring.

One approach that has shown promise for demonstration of direct capture, identification, and quantitative assessment of pathogenic organisms for use in a rapid first alert detection scheme has been that of peptide-functionalized microfabricated chips (Zhang, 2004; Dhayal, 2006). Here, cantilever array chips are functionalized with short peptides known to be specific for *Bacillus subtilis* spores. A microfluidic system is employed to direct a solution containing the target species to the cantilever arrays. The *Bacillus subtilis* spores attach to the cantilevers, and the resonance frequency of the cantilevers is subsequently reduced in a measurable fashion as the mass of the cantilever plus spore system increases. While this approach provides a method for quantitative detection with a high degree of discrimination, it is very sensitive to the properties of the suspension fluid and lacks an ability to destroy the target species once they are identified.

The use of nanoshells in biodetection

A relatively new approach to biodetection utilizes a novel class of optically tuneable nanoparticles called nanoshells (Bertin, 2006; Mortensen, 2006; Dillenback, 2006; Souza, 2006). These consist of a dielectric core surrounded by a thin gold shell (see Figure 1). One highly desirable property of nanoshells is that they can be custom designed to scatter and/or

Figure 1. Schematic illustration of a nanoshell.
Schematic illustration of a nanoshell showing the silica dielectric core (~100 nm), and the gold shell (<30 nm).

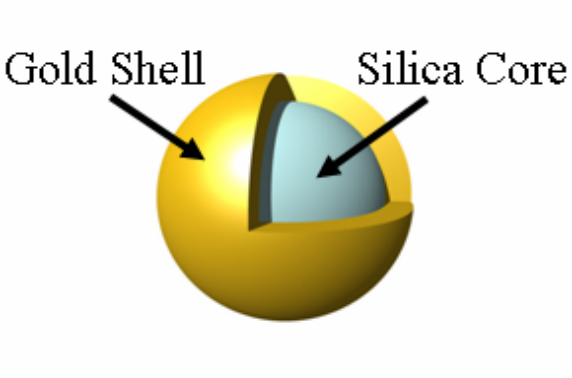
Gold Shell
Silica Core

absorb light over a broad spectral range (Jackson, 2003; Oldenburg, 1999). This range includes the near-infrared (NIR), a wavelength region of particular interest because it provides maximal penetration of light through tissue.

The absorption and scattering properties of the nanoshells is due to existence of a surface plasmon resonance, and is controlled by tailoring the relative dimensions of the shell thickness and core radius. While the underlying physical principles of surface plasmon resonance are complex, an adequate working knowledge of the technique does not require a detailed theoretical understanding. A light source shown on a metal surface will induce waves of electrons, or plasmons, at the surface of the metal. Surface plasmons, which are sometimes referred to as surface polaritons, are surface electromagnetic waves that propagate in parallel along a metal/vacuum or metal/dielectric interface. Because the wave is on the boundary of the metal and the external medium (air or some solution, for example), these oscillations are very sensitive to variations of the properties of this boundary. As the dimensions of this interface shrink to the point where they are on the order of the plasmon, a resonance occurs, and the plasmon becomes like a standing wave. This leads to an enhancement in the absorption properties at the excitation wavelength.

In the work of Loo et al. (Loo, 2005; Wang, 2005), nanoshells designed to have a high scattering optical cross-section were conjugated with anti-HER2 antibodies, and then these biofunctionalized nanoshells were incubated with HER2-positive SKBr3 breast adenocarcinoma cells. When the

cells were imaged under a darkfield microscope sensitive to scattered light, the images clearly show increased scatter-based optical contrast due to nanoshells binding to the surface of the adenocarcinoma cells as compared to the control cell group which were free of nanoshells. Hirsch et al. (Hirsch, 2003; O'Neal, 2005) utilized the NIR absorption properties as a novel means to mediate photothermal ablation of cancer cells decorated with immunotargeted nanoshells. These and other approaches (Jiang, 2005; Lin, 2005) suggest numerous emerging implications of biologically enhanced nanotechnology in medical diagnostics and therapeutics (Cuenca, 2006; Loo, 2005; You, 2005; Kalele, 2006; Rozenzhak, 2005).

Examination of biofunctionalized nanoshells at the microscopic scale

It is of interest to consider the details of application of biofunctionalized nanoshells immunotargeting other biological targets, for example, bacterial cells and bacteriophage . Specifically, a correlation between what is occurring at the microscopic scale to that observed on the macroscopic scale would provide insight into the mechanism(s) involved in techniques such as enhanced optical contrast as well as photothermal ablation. The nanoshells themselves can be designed to strongly absorb NIR light of a desired wavelength. Further, antibodies specific for most bacterial cells of interest are readily available. However, bacterial cells, spores, and bacteriophage all have orders-of-magnitude smaller surface areas and volumes than, for example, breast adenocarcinoma cells. It is, therefore, unclear if the

approach demonstrated by Loo et al. (Loo, 2005) and Hirsch et al. (Hirsch, 2003) will be successful with these significantly smaller and much more mobile targets. In this research effort, we explore the ability of nanoshells functionalized with biomolecular recognition to neutralize individual *Escherichia coli* bacterial cells, *Bacillus subtilis* spores, and bacteriophage targets when excited by a controlled dose of near-IR irradiation. Microscopic imaging techniques are employed to evaluate both pre- and post-irradiation of biofunctionalized and control *Escherichia coli* bacterial cells with NIR laser radiation. The microscopic results obtained from electron microscopy are compared to *Escherichia coli* viability after exposure to appropriately excited biofunctionalized nanoshells. In addition, the effect of IR irradiation on the viability of *Escherichia coli* bacteriophage with a demonstrated affinity for gold nanoshells is also measured. Finally, we briefly consider extension of the technique to the use of short peptide ligands as capture elements, and examine their suitability for detection and destruction of *Bacillus subtilis* spores, a simulant of *Bacillus anthracis* spores (Dhayal, 2006), the causative agent of anthrax. This research extends the choice of biological recognition motif to short peptides which have advantages over antibodies in certain aspects of manufacturing and design control.

II. MATERIALS AND METHODS

Gold nanoshell fabrication

Nanoshells consisting of a silica core and a gold coating are designed to have peak optical scattering and absorption efficiencies in the NIR (~800 nm). The silica nanoparticles were fabricated using the Stöber method (Stöber, 1968). Here, a system of chemical reactions is utilized which permits the controlled growth of spherical silica particles of uniform size by means of hydrolysis of alkyl silicates and subsequent condensation of silicic acid in alcoholic solutions. Ammonia is used as a morphological catalyst. Solutions generated are monodisperse suspensions of silica spheres in the colloidal size range of from less than 50 nm to over 2 μm.

Once fabricated, the silica nanoparticle surface was then terminated with amine groups by reaction with (aminopropyl)triethoxysilane (APTES). The gold shell was grown by first nucleating gold colloid using the method of Duff and Baiker (Duff, 1993), and then allowing the colloid to absorb onto the aminated silica nanoparticle surface. Additional gold was then reduced onto these colloid nucleation sites using potassium carbonate and $HAuCl_4$ in the

presence of formaldehyde. Nanoshells were fabricated with dimensions shown in Figure 2. This provided a peak optical scattering and absorption at our target wavelength of 808 nm. The theoretical and measured spectral characteristics of the scattering/absorbing nanoshells as measured by a UV-Vis-IR spectrophotometer are shown in Figure 3. Figure 4 shows a scanning electron microscopy (SEM) image of the nanoshells fabricated in this fashion.

Figure 2. Schematic of nanoshell dimensions.

Schematic showing the radius of the dielectric and the dielectric plus gold coating. The plus-or-minus (+/-) in the figure is experimentally determined from the variation of the width of the absorption spectra as compared to the theoretically predicted surface plasmon resonance absorption of nanoshells. The density of nanoshells in stock solution was determined by UV-Vis spectrophotometry to be 1.1×10^{10} nanoshells ml^{-1}. The size distribution and particle density are measured after each colloid solution of gold coated nanoshells are synthesized.

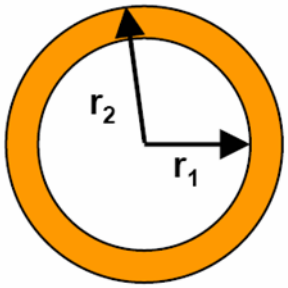

$r_1 = 65 \pm 6.2$ nm

$r_2 = 78 \pm 3$ nm

concentration:

1.1×10^{10} particles/mL

Figure 3. Plot of absorption spectra.

Plot comparing the theoretical and measured absorption of the gold coated nanoshells as determined by UV-Vis spectrophotometry. The abscissa is the wavelength of absorption, while the ordinate is the relative absorption of the nanoshells at that excitation wavelength.

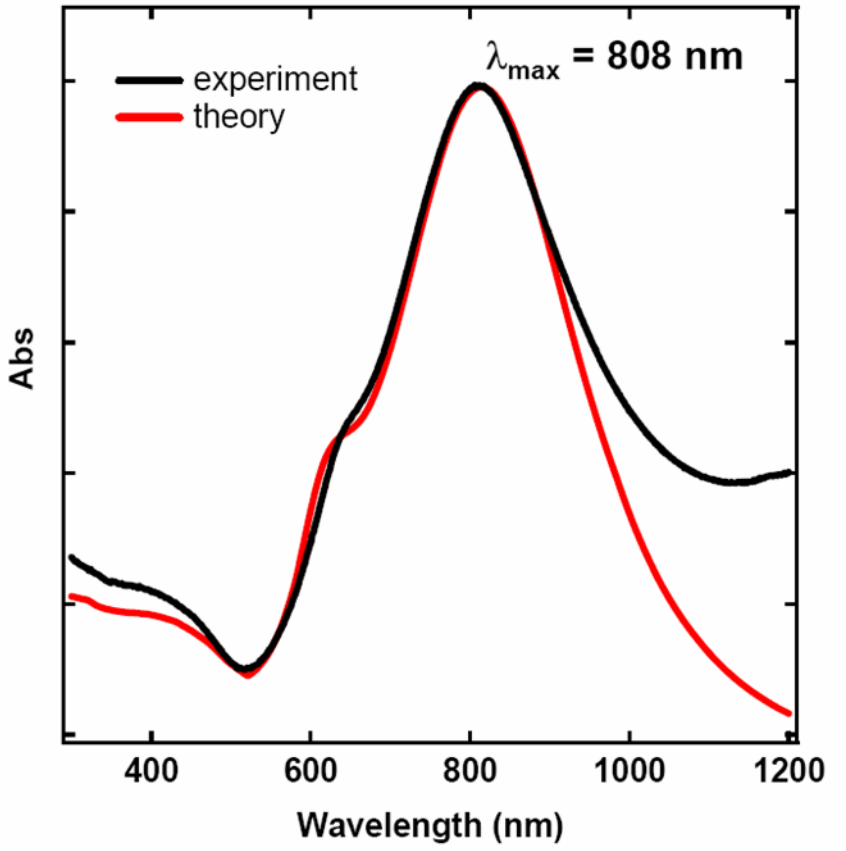
λmax = 808 nm
experiment
theory
Abs
400
600
800
1000
1200
Wavelength (nm)

Figure 4. Scanning electron microscopy image of nanoshells.

Scanning electron microscopy image of gold coated nanoshells taken using secondary electron imaging, an excitation voltage of 20 kV, and a working distance of 5.4 mm. The stock nanoshell solution is spotted from stock solution onto silicon substrate, and vacuum dried prior to imaging. The drying process causes the nanoshells to appear somewhat clustered.

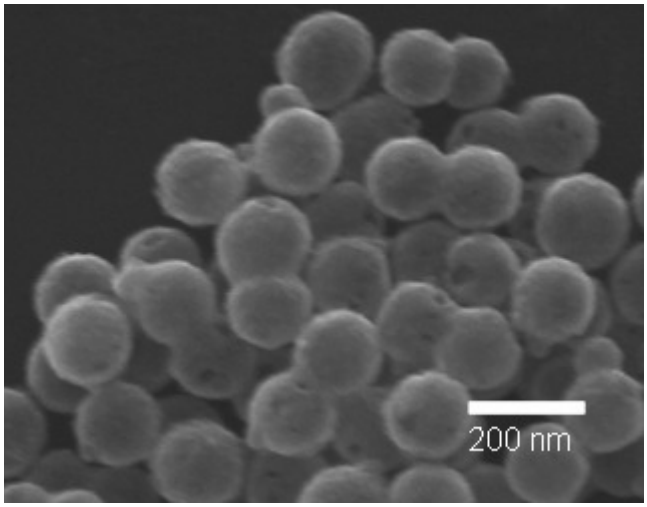
200 nm

Antibody and short peptide conjugation

Rabbit polyclonal IgG antibodies to *Escherichia coli* from Abcam Inc. (ab13626) are used to biofunctionalize the gold nanoshells to recognize and bind to *Escherichia coli*. According to the manufacturer, this antibody reacts with all "O" and "K" antigenic serotypes of *Escherichia coli*. The antiserum is not absorbed for other members of the Enterobacteriaciae. The antibodies are dispersed in deionized water and incubated with the gold nanoshells. Attachment to the gold nanoshells is achieved through the amino groups present on the antibodies. The amino group has an affinity for gold, and incubation of the antibodies with gold coated nanoshells results in biofunctionalized nanoshells. The biofunctionalized nanoshells are then centrifuged at 450 rcf for 5 minutes at 4ºC. The supernatant is decanted off and the biofunctionalized nanoshells are resuspended in water with a vortex. This washing procedure is repeated two more times in order to remove any unbound antibodies.

A similar approach is utilized for attachment of short peptides to the gold nanoshells. The commercial short peptide sequences utilized are synthesized by standard solid-phase peptide synthesis and characterized by high-performance liquid chromatography (HPLC) and electrospray ionization mass spectrometry. The short peptide sequences used are NHFIVSPKPNEM-GGGC (BS1) and NHFLPKV-GGGC (BS2). Both of these sequences have been demonstrated to efficiently capture *Bacillus subtilis* spores in solution (Dhayal, 2006). Another peptide sequence,

NHDYKDDDDKPAYSSGAPPMPPFC (Flg-A3C), that has no affinity for *Bacillus subtilis* was also utilized as a control. Attachment of the short peptides to the gold nanoshells is achieved by first centrifugation of the nanoshells solution at 450 rcf for 5 minutes at 4ºC. Then, the supernatant is decanted off and the nanoshells are resuspended in 0.1 M $NaHPO_4$ buffer with pH = 9.0. A stock solution of peptide is prepared by dissolving 10 mg of lyophilized peptide (from New England Peptide) in 1.0 ml of doubly deionized water to yield a peptide concentration of 10 mg ml^{-1} or 2.44×10^{-3} M. For conjugation, 5.0 ml of short peptide (1.22×10^{-8} moles) is then added to the nanoshells in $NaHPO_4$ buffer, which results in deprotonation of the cysteine residue. This enhances the rate of thiol bond formation between the cysteine residue and the gold surface of the nanoshell, resulting in biofunctionalized nanoshells. After incubation, the unbound peptides are washed off in the same fashion as for the antibodies described above. In order to verify attachment of the peptides to the nanoshells, FTIR measurements are performed on the pure peptide and the biofunctionalized nanoshells. As shown in Figure 5, the S—H stretching mode at ~2600-2700 cm^{-1} of the cysteine residue is present in the short peptide, but absent in the peptides bound to the gold nanoshell. This gives us some confidence that the peptides are bound to the gold by a thiol linkage via the cysteine residue.

Figure 5. FTIR data of short peptide.

FTIR measurements of the pure peptide and of peptide bound to gold nanoshells. The abscissa is the wavenumber of the incident light, and the ordinate is the percent of incident light of that wavenumber that is transmitted through the sample.

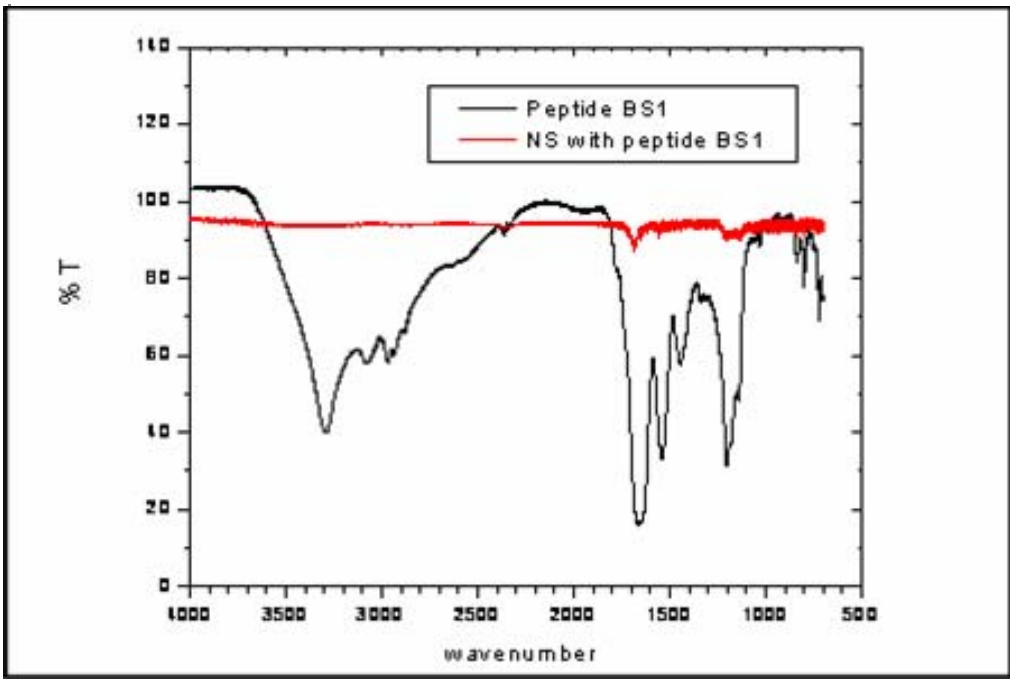
Peptide BS1
NS with peptide BS1
% T
wavenumber
140
120
100
80
60
40
20
0
4000
3500
3000
2500
2000
1500
1000
500

Escherichia coli bacterial cell cultures and *Bacillus subtilis* spores

Escherichia coli K12 strain ER2738 (New England BioLabs Catalog No. E4104S) bacterial cells are cultured by first streaking out stock K12 stored at -80ºC onto a Luria-Bertini (LB) petri plate and incubating them overnight at 37ºC. A single colony of *Escherichia coli* is then transferred to LB broth, and cultured overnight in a shaking incubator at 37ºC. Control tubes of LB broth that have not been inoculated with *Escherichia coli* are used in parallel with the cultures to verify there is no contamination. After overnight growth, 30 µl of overnight culture is transferred to 3 ml of sterile LB broth, and allowed to culture in a shaking incubator at 37ºC for an additional 4 hours. This results in a concentration of ~7 x 10^6 ml^{-1} as determined by optical density measurement at 600 nm. The optical density measurements are taken using a Cary 500 Scan UV-Vis-IR spectrophotometer set to measure the optical density of the test solution (after background subtraction) for an excitation wavelength of 600 nm. Here, and optical density of 1.0 corresponds to 1.0×10^7 cells ml^{-1}. A 1.0 ml volume of culture is then transferred to an Eppendorf tube and centrifuged at 6800 rcf for 5 minutes at 4ºC. The *Escherichia coli* forms a pellet at the bottom of the Eppendorf tube. The supernatant is decanted off, and the *Escherichia coli* is resuspended in deionized water using a vortex. This step is repeated two more times in order to wash the LB off the *Escherichia coli*. The resulting *Escherichia coli* are then incubated overnight at 4ºC with the appropriately biofunctionalized nanoshells or control in preparation for further study.

Bacillus subtilis (ATCC No. 6633) spores suspended in 40% ethanol in deionized water were obtained from Raven Biological Laboratories, Inc. The spores were evaluated by SEM as shown in Figure 6, and determined to have a concentration of 3.7×10^3 CFU ml^{-1} in good agreement with the manufacturers performance data sheet.

Figure 6. Scanning electron microscopy image of *Bacillus subtilis* spore.

Scanning electron microscopy image of *Bacillus subtilis* spore.

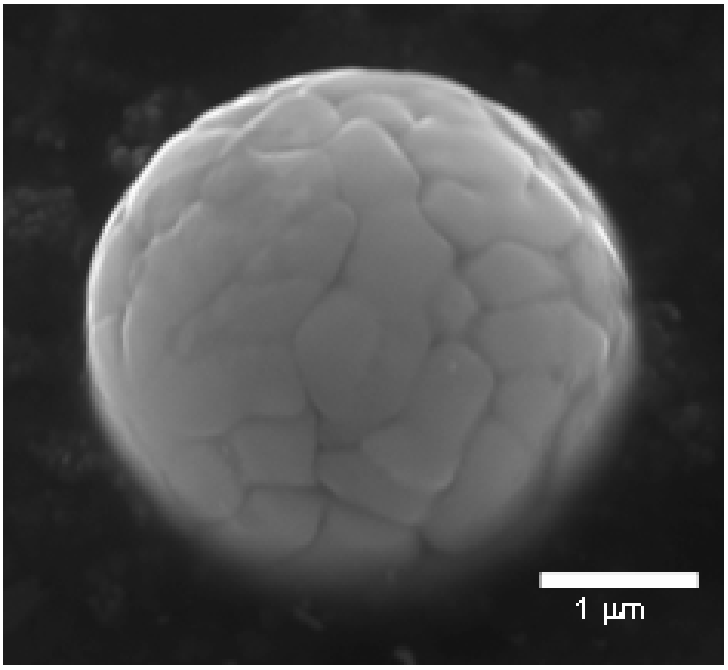
1 µm

Near infrared laser irradiation

The near infrared radiation is provided by an AlGaAs/GaAs multi-quantum well semiconductor laser diode operated with an optical flux of 1 W cm^{-2} power and a fundamental mode wavelength of 808 nm. The laser is operated in constant current mode, and a thermoelectric cooler is used to maintain temperature stability of the laser diode. Power is found to drift by less than 3% over a 2 hour period. A schematic of the laser diode and sample exposure system is shown in Figure 7. The operation of the laser is computer controlled and uses the computer system clock for exposure time. The nanoshells are designed to have peak optical scattering and absorption at a wavelength of 808 nm so that they will have maximum coupling to the laser radiation. The Au nanoshells possess a large photothermal response, and have been shown to exhibit thermal transfer over nanometer length scales via thermally sensitive molecular linkers (Slocik, 2007). A significant enhancement of the photothermal response has also been reported for pairs and clusters of nanoshells due to resonance enhancement of groups of nanoshells over single nanoshells (Prodan, 2003).

Figure 7. Schematic of laser diode apparatus.

Schematic of AlGaAs/GaAs laser diode apparatus used to expose biological samples to 808 nm NIR radiation.

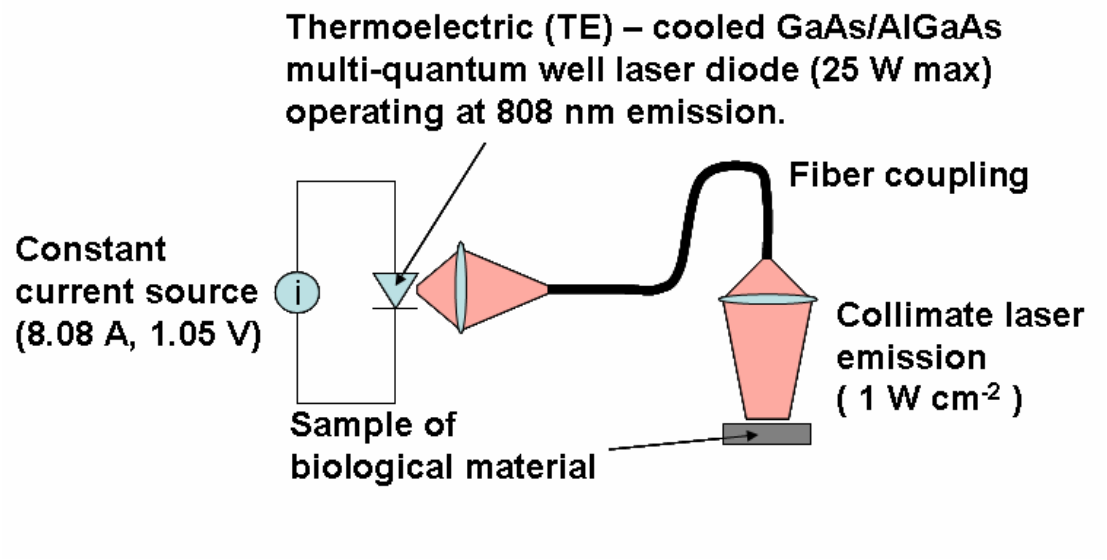
Thermoelectric (TE) – cooled GaAs/AlGaAs multi-quantum well laser diode (25 W max) operating at 808 nm emission.
Fiber coupling
Constant current source (8.08 A, 1.05 V)
i
Collimate laser emission (1 W cm-2)
Sample of biological material

Bacteriophage nanoshells binding and elution procedure

Two different bacteriophage, one from Ph.D.-7 and -12 Phage Display Peptide Library Kits from New England BioLabs are utilized in this research effort, both of which have demonstrated an affinity for gold nanoshell surfaces as will be shown later. Both the Ph.D. -7 and -12 library kits are based on a combinatorial library of random peptide 7- and 12-mers, respectively, fused to a minor coat protein (pIII) of M13 phage. Phage display is a technique in which a peptide or protein is expressed as a fusion with a coat protein of a bacteriophage, resulting in display of the fused protein on the surface of the virion, while the DNA encoding the fusion resides within the virion. In its simplest form, panning is carried out by incubating a library of phage-displayed peptides with the desired target, washing away the unbound phage, and then eluting the specifically-bound phage from the target. This process is described in Figure 8. The eluted phage is then amplified in *Escherichia coli* culture and taken through additional binding/amplification cycles to enrich the pool in favor of enhanced binding sequences. After 3-4 rounds, the individual clones are characterized by DNA sequencing. Note that M13 is not a lytic phage, so plaques obtained from the purified clones are due to diminished cell growth rather than cell lysis.

Utilizing the Ph.D. combinatorial library kits, two M13 bacteriophage clones have been identified as having an affinity to gold nanoshells. The first M13 clone, which is referred to as NS-73, contains the 7-mer peptide sequence IGLPYPA fused to the pIII minor coat protein of the M13 phage.

The second M13 clone, which is referred to as NS-32, contains the 12-mer peptide sequence TIIMDQRPPTHL fused to the pIII minor coat protein of the M13 phage. Binding of either of these bacteriophage to the gold nanoshells is achieved simply by incubating the nanoshells with the bacteriophage overnight in the 4ºC refrigerator. The ratio of nanoshells to bacteriophage is controlled by performing serial dilutions of bacteriophage while keeping the nanoshells concentration constant. After exposure to 808 nm laser radiation, the bacteriophage are eluted from the nanoshells by combining the bacteriophage functionalized nanoshells with 1 ml of 0.2 M glycine-HCl (pH=2.2), and using rotation mixing for 5 minutes. Then, the solution is neutralized using 150 µl of 1 M TRIS-HCl (pH=9.1) followed by vortexing at low speed so that the bacteriophage are not damaged. The control samples that are not exposed to IR radiation are eluted in this fashion as well.

Figure 8. Schematic of panning with the Ph.D. peptide library.

Schematic of the panning process employed in the Ph.D. Phage Display Peptide Library Kit from New England BioLabs. Panning is carried out by incubating a library of phage-displayed peptides with the desired target, washing away the unbound phage, and eluting the specifically bound phage. The eluted phage is then amplified and taken through additional binding/amplification cycles to enrich the pool in favor of binding sequences (New England BioLabs, 2002)

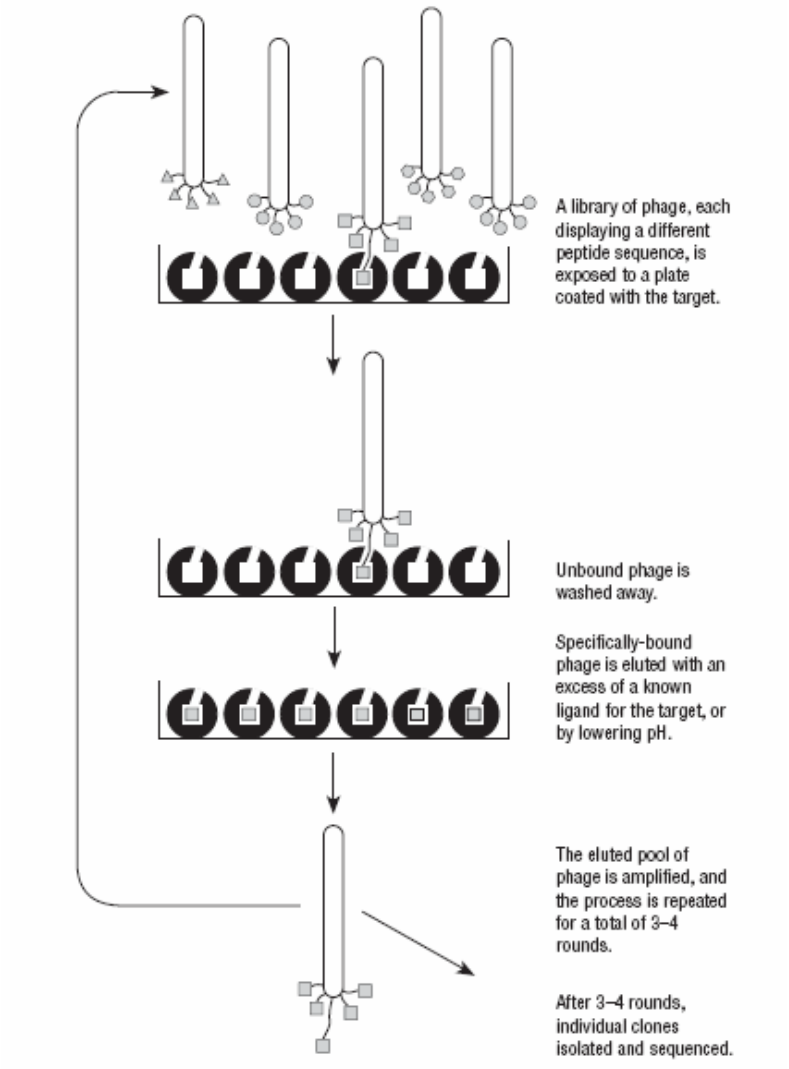
A library of phage, each displaying a different peptide sequence, is exposed to a plate coated with the target.
Unbound phage is washed away.
Specifically-bound phage is eluted with an excess of a known ligand for the target, or by lowering pH.
The eluted pool of phage is amplified, and the process is repeated for a total of 3–4 rounds.
After 3–4 rounds, individual clones isolated and sequenced.

Bacteriophage Titering Procedure

The phage titering begins with preparation of an overnight culture. Pick a colony of non-competent K12 *Escherichia coli* bacteria using a sterile tooth pick. Dip the tip of the tooth pick in 3 ml of LB broth, and leave overnight in the shaking incubator at 37ºC. The next morning, prepare a 1:100 dilution day culture by adding 30 µl of the overnight culture to 3 ml of sterile LB broth, and leave in the shaking incubator at 37ºC until the culture reaches mid-log phase. Next melt top agarose and distribute 4 ml into 15 ml conical tubes, and store in water bath at 60ºC until needed. Remove LB plates from 4ºC refrigerator and warm in 37ºC incubator approximately an hour before use. The infection process begins by taking 200 µl of day culture in a 1.5 ml Eppendorf tube, and infecting with 10 µl of the phage dilution whose concentration you are trying to determine. Allow the inoculated *Escherichia coli* to incubate for about 5 minutes. While the phage and *Escherichia coli* are incubating, pull the LB plates from the incubator and the liquid top agarose from the water bath. To the top agarose add 4 µl of 1 M IPTG and 40 µl of XGAL and vortex. Then, add the infected bacteria to the agarose tube, vortex, and pore out onto the LB plate. Distribute the agarose evenly using a figure eight motion, and allow solution to gel before storing in the 37ºC incubator overnight. The blue plaques can be counted the next day, and the number of plaque forming units calculated.

Table 1. Nomenclature cross reference.

Correlation of sample names with strains and relevant technical information for samples described in this thesis.

Sample Name	Strain	Source	Comments
Bacillus subtilis	ATCC No. 6633	Raven Biological Laboratories	Batch 6633-4
Escherichia coli	ER2738	New England BioLabs	K12, Cat. No. E4104S
NS-73	M13	New England BioLabs Ph. D.-7 Phage Display Peptide Library Kit	Nanoshell consensus sequence: IGLPYPA
NS-32	M13	New England BioLabs Ph. D.-12 Phage Display Peptide Library Kit	Nanoshell consensus sequence: TIIMDQRPPTHL

III. RESULTS

Biofunctionalized nanoshells and their attachment to *Escherichia coli*

A schematic diagram describing the coupling of antibodies to the gold nanoshell, targeting to *Escherichia coli*, and transferring energy from IR radiation to the target species is shown in Figure 9. Polyclonal IgG antibodies specific to *Escherichia coli* were conjugated to the surface of the gold nanoparticles by incubation of the antibodies with the nanoshells. Attachment of the antibodies to the nanoshell surface occurs through the amino groups present in the antibodies reacting with the gold on the surface of the nanoshell (Kalele, 2006).

Attachment of biofunctionalized nanoshells to *Escherichia coli*

A scanning electron microscopy image of *Escherichia coli* bacteria incubated with rabbit polyclonal antibody biofunctionalized nanoshells is shown in Figure 10. Nanoshells are clearly observed to be bound to *Escherichia coli*. Biofunctionalization of the nanoshells tends to cause the formation of some clustering of the nanoshells. This is believed to be due to hydrogen bonding, and the bonds are easily disrupted by vortexing or

ultrasonication. This can occur in groups as small as two or three nanoshells, or in larger clusters as shown in the collage of Figure 10B. The bacterial cells were in excess compared to the concentration of biofunctionalized nanoshells, and no unbound nanoshells were observed to be present in the open areas between bacterial cells. In order to evaluate the effect of low concentrations of nanoshells on the *Escherichia coli* bacterial cells, the concentration of nanoshells was kept small in comparison to the concentration of bacterial cells. Nanoshells were also commonly observed to be bound to two or more bacterial cells at once, acting as a binding agent between the cells.

The bound nanoshells could not be washed off using deionized water, and *Escherichia coli* bacteria were readily pulled down out of solution when centrifuged at only 450 rcf for 5 minutes, the same centrifuge condition used for unbound nanoshells.

Figure 9. Schematic of biofunctionalization, recognition, and neutralization of target species.

Schematic representation of conjugation of nanoshells with antibodies, antibody-epitope recognition, exposure to IR radiation and transfer of energy causing lysing of target species.

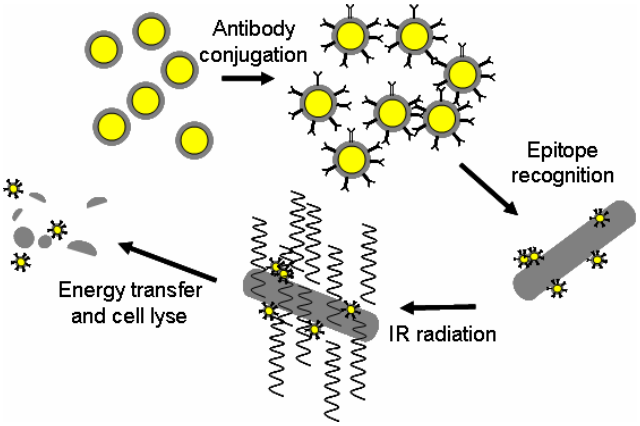
Antibody
conjugation
Epitope
recognition
IR radiation
Energy transfer
and cell lyse

Figure 10. Scanning electron microscopy images of *Escherichia coli* with nanoshells.

Scanning electron microscopy image of *Escherichia coli* bacteria incubated with rabbit polyclonal antibody biofunctionalized nanoshells. (A) Individual *Escherichia coli* with nanoshells in higher resolution image. (B) Four panel collage of scanning electron microscopy images showing different numbers of nanoshells bound to *Escherichia coli*. The scale bars shown in each panel are 1 μm in length.

Figure 10 A

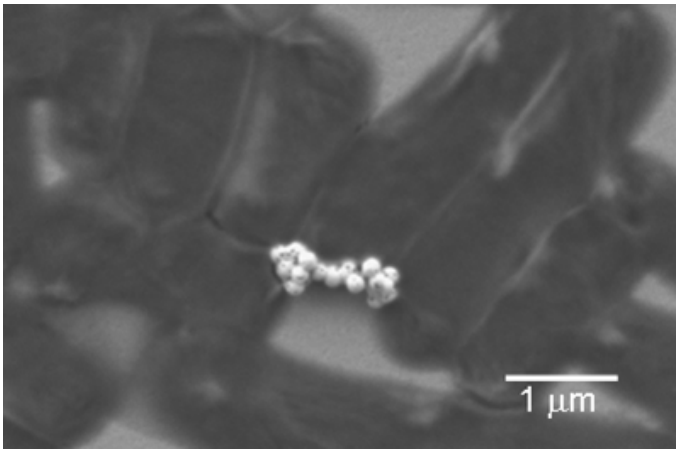

Figure 10 B

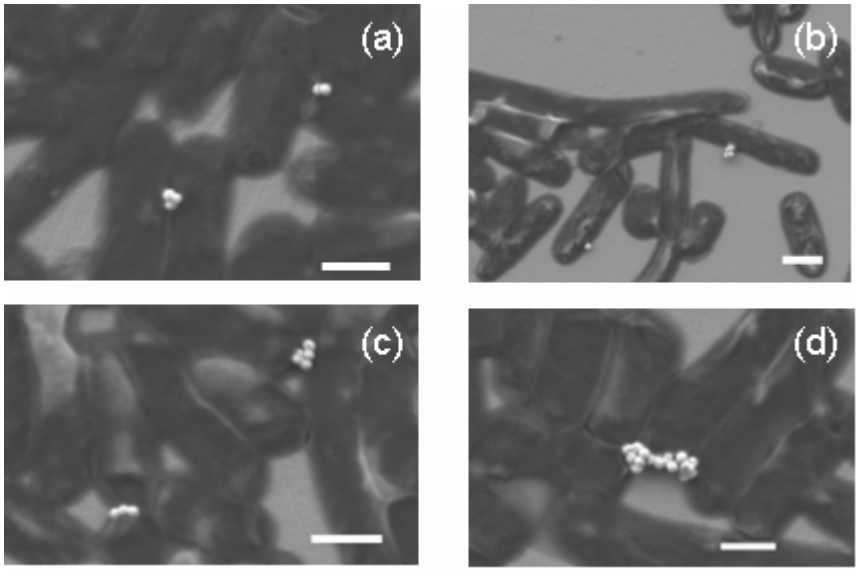

Effect of exposure to IR radiation on *Escherichia coli*

The results for exposure of the *Escherichia coli* bacterial cells incubated with rabbit polyclonal antibody biofunctionalized nanoshells to IR radiation is shown in Figure 11. The energy absorbed by the nanoshells appears to be transferred to the target species. The IR irradiation has clearly caused damage to the *Escherichia coli* bacterial cells. This can be seen by the change in the morphology of the bacterial cell, which appears to have lysed. However, based on these experiments, it was not possible to determine if the antibodies conjugated to the nanoshell acted to transfer the thermal energy to the target species, or if they only functioned to momentarily tether the nanoshell in the vicinity of the cell, and subsequent random motion provided the necessary thermal contact. The nanoshell that was originally attached to the bacterial cell wall can still be seen in lower right of the image. Further, the other bacterial cells present in the image which lack attachment to biofunctionalized nanoshells have been subjected to the same preparation and IR exposure protocol, and yet show no visible effects, such as causing the cells to lyse, to the radiation. One also observes that, after IR exposure, the nanoshells were often found to be nearby but detached from the damaged cells. This may be due to a change in the conformation of the epitope on the cell surface that the antibody would normally attach to, or possibly to a lack of cell surface in general.

Figure 11. Scanning electron microscopy image showing results of infrared irradiation of *Escherichia coli* decorated with biofunctionalized nanoshells. Scanning electron microscopy image of *Escherichia coli* bacteria incubated with rabbit polyclonal antibody biofunctionalized nanoshells that have been exposed to 808 nm radiation for 5 minutes at 1 W cm^{-2}. (A) Individual *Escherichia coli* with nanoshells exposed to IR radiation in higher resolution image. Cell appears to have been damaged and to lyse as a result of the combination of the presence of a biofunctionalized nanoshell and exposure to IR irradiaton. The *Escherichia coli* bacterial cells to left and bottom of the lysed cell have been exposed to the same IR irradiation, but do not appear to have lysed. (B) Nine panel collage of images showing different *Escherichia coli* that were bound to either individual or small clusters of biofunctionalized nanoshells and exposed to IR radiation. The scale bars shown in each panel are 1 μm in length.

Figure 11 A

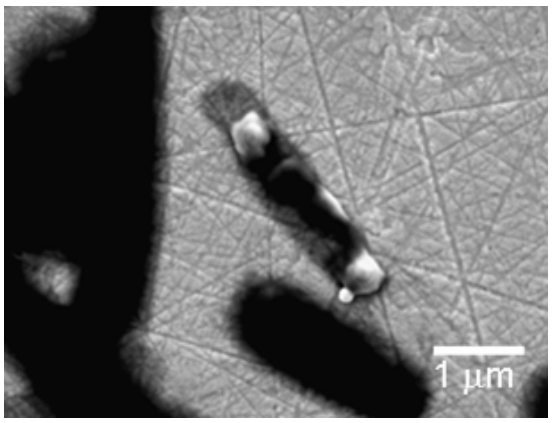

Figure 11 B

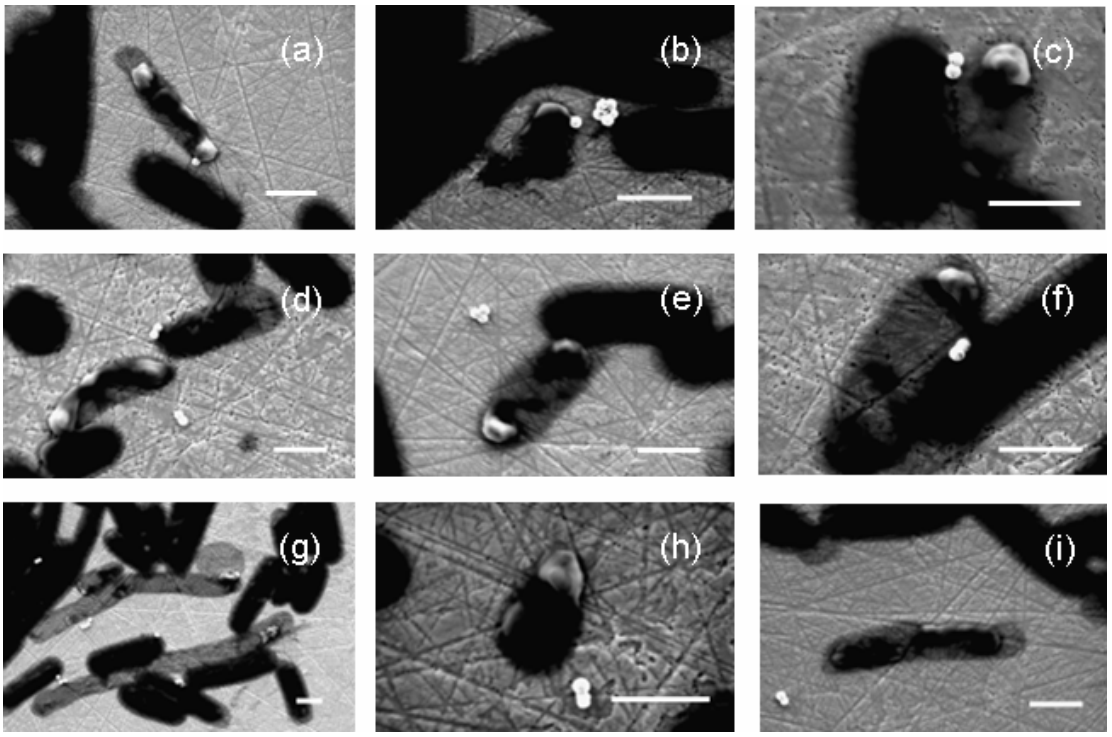

As a control, *Escherichia coli* cells were prepared in a parallel fashion to those shown in Figure 11, but were not incubated with biofunctionalized nanoshells. A scanning electron micrograph of these cells after they were exposed to 808 nm IR radiation of the same dose is shown in Figure 12. These cells show no change in morphology, and at least some of the cells proved viable as determined by the appearance of colonies when a sample of the cells in Figure 12 were streaked out on onto a Luria-Bertini (LB) petri plate and incubated overnight at 37ºC.

IR exposure of *Escherichia coli* in solution

In order to evaluate the effect of the infrared radiation on the target species, samples of *Escherichia coli* in PBS buffer were prepared under three different conditions. The first condition was that of only *Escherichia coli* in buffer without any nanoshells present. The second condition was that of including nanoshells in the PBS buffer with the *Escherichia coli*. The last condition utilized biofunctionalized nanoshells in the PBS buffer with the *Escherichia coli*. These samples were each exposed to 808 nm IR radiation for 5 minutes at 1.0 W cm^{-2}. The results for these experiments are shown in Figure 13. From Figure 13, we see the concentration of viable bacteria was essentially unaffected by exposure to the IR radiation in the absence of nanoshells.

Figure 12. Scanning electron microscopy image of *Escherichia coli* subject to IR radiation.

Scanning electron microscopy image of *Escherichia coli* bacteria without nanoshells subject to the same sample preparation protocol used for the *Escherichia coli* used in Figure 11 but with double distilled water used in place of the nanoshell solution, and exposed to 808 nm radiation for 5 minutes at 1 W cm^{-2}.

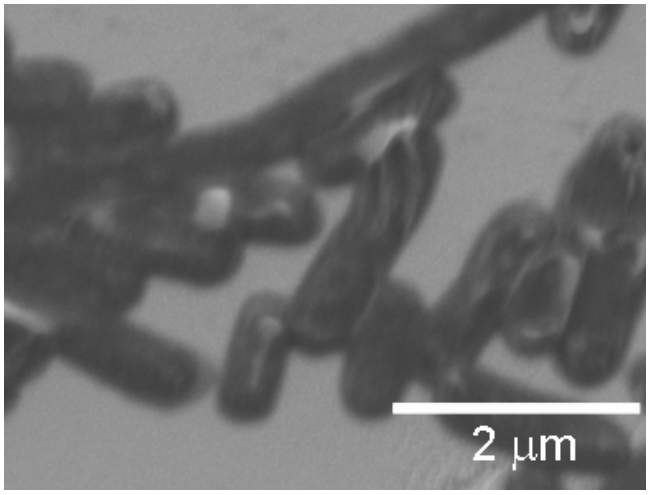
2 μm

Figure 13. Plot of *Escherichia coli* exposed to IR radiation.

Plot of the change in colony forming unit (CFU) concentration of *Escherichia coli* exposed to IR radiation under the conditions of no nanoshells, nanoshells free of antibodies, and biofunctionalized nanoshells. The original concentration of *Escherichia coli* is 1.36×10^{6} CFU ml^{-1}. All experiments were performed in triplicate, and the error bars represent the standard deviation of the results from the mean. A ratio of ~10^{5} nanoshells per CFU of *Escherichia coli* was utilized for this set of experiments.

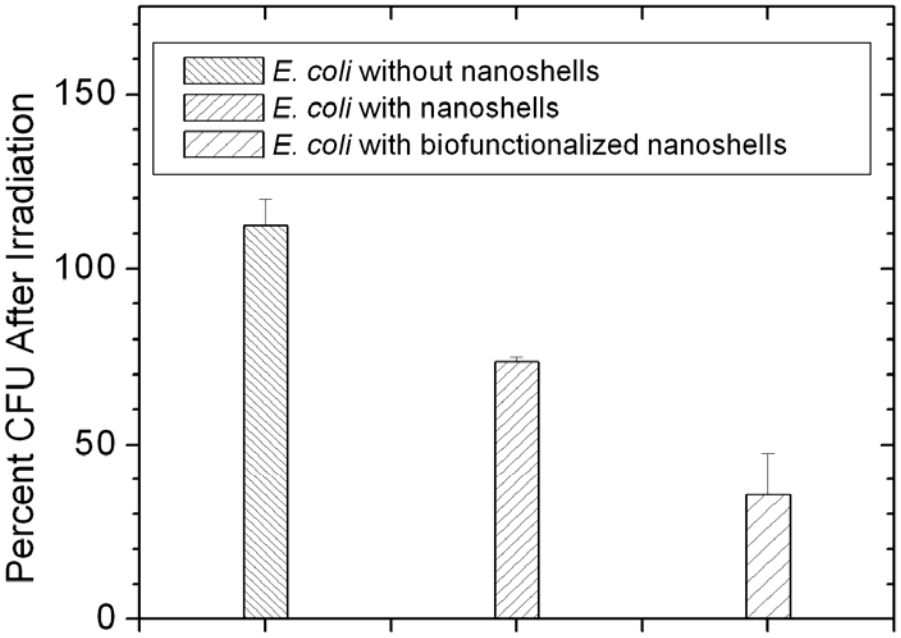
E. coli without nanoshells
E. coli with nanoshells
E. coli with biofunctionalized nanoshells
Percent CFU After Irradiation
150
100
50
0

It should here be noted that the IR radiation was observed to pass through the entire volume of the PBS buffer as indicated by a phosphorescent material located under the Eppendorf tube containing the volume of test material. This tells us that all the bacteria in the PBS buffer were exposed to the IR radiation, and not just those near the surface.

The presence of antibody-free nanoshells with the *Escherichia coli* in the PBS buffer resulted in a measurable decrease in the population of viable *Escherichia coli*. This is believed to be due to random contact between the nanoshells that have been heated by the IR radiation and bacterial cells in their local vicinity. This incidental contact would be a non-specific form of nanoshell-bacterial cell interaction. Finally, Figure 13 shows the biofunctionalized nanoshells which had been decorated with antibodies specific for *Escherichia coli* were found to cause most of the bacterial cells to become non-viable. This result, consistent with scanning electron microscopy of nanoshells binding to *Escherichia coli* bacterial cells, leads us to believe that the nanoshells are at least temporarily localized to the bacterial cells by the antibodies, and that this localization enhances the likelihood of a transfer of thermal energy from the nanoshell to the target species during IR irradiation. This is somewhat surprising when one considers the extremely small size of an antibody in comparison to both the nanoshell and the *Escherichia coli* bacterial cell, as well as the type of bonding mechanism between the antibody and its epitope.

Attachment of M13 bacteriophage to nanoshells

Additional biological targets explored in this research are two M13 bacteriophage that are specific for *Escherichia coli*. The first is labeled NS-73, and is an M13 bacteriophage that is specific for *Escherichia coli*. This bacteriophage was panned from a 7 mer phage display peptide library as described in the Materials and Methods section, and shows an affinity for Au nanoshells. The second is labeled NS-32, and is also an M13 bacteriophage specific for *Escherichia coli*, but was panned from a 12 mer library against gold nanoshells. Figure 14 shows an image of M13 bacteriophage described in the Materials and Methods section of this thesis. The three panel collage in Figure 14 shows several M13 bacteriophage whose pIII minor coat protein have an affinity for gold nanoshells. The images of the M13 bacteriophage bound to nanoshells are taken using low voltage transmission electron microscopy. A number of these bacteriophage are seen to be bound to nanoshells.

Figure 14. TEM image of M13 bacteriophage.

Three panel collage of M13 bacteriophage that have a minor coat protein (pIII) which has an affinity for gold nanoshells. The images of the M13 bacteriophage bound to nanoshells are taken by low voltage transmission electron microscopy. The length of the bars are as shown in each image.

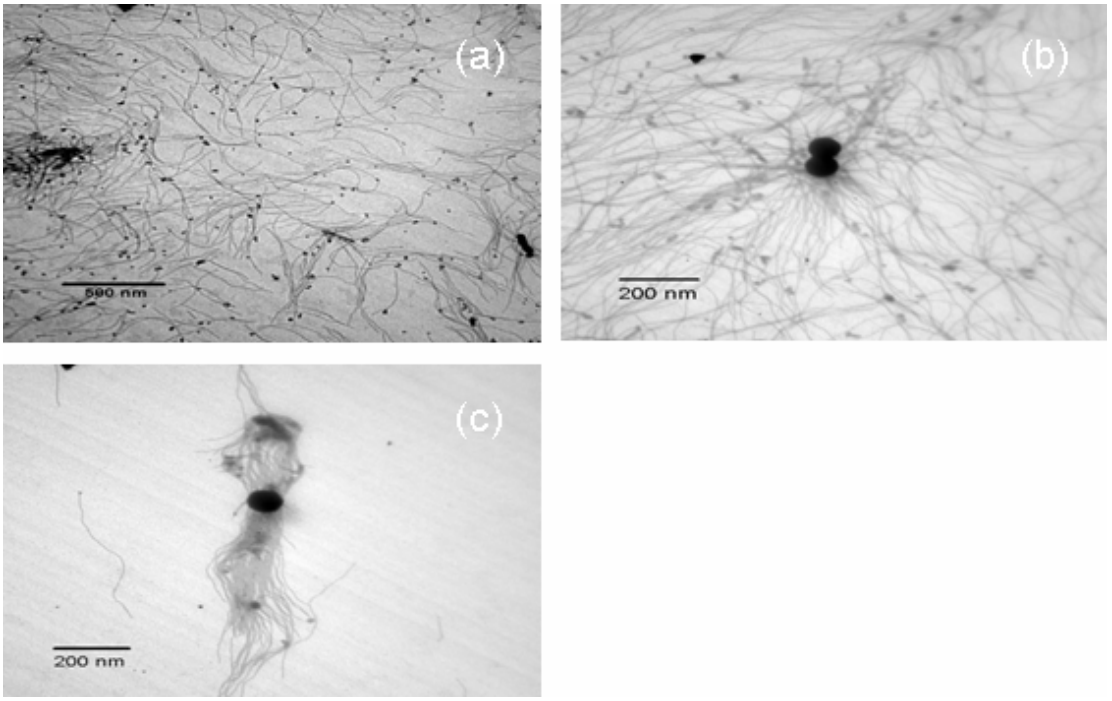
(a)
500 nm
(b)
200 nm
(c)
200 nm

IV. DISCUSSION

Attachment of biofunctionalized nanoshells to target species

Recall from the introductory section of this thesis that one of the objectives of this research was to determine if biofunctionalized nanoshells would bind to biological targets that are much smaller than the HER2-positive SKBr3 breast adenocarcinoma cells of earlier studies. Based on the electron microscopy images shown earlier, the biofunctisonalized nanoshells show a preference to being bound to their respective target species. Furthermore, the energy absorbed by the nanoshells appears to be transferred to the target species. This energy transfer then results in a lysing of the cell wall. However, based on these experiments, it was not possible to determine if the antibodies conjugated to the nanoshell acted to transfer the thermal energy to the target species, or if they only functioned to momentarily tether the nanoshell in the vicinity of the cell, and subsequent random motion provided the necessary thermal contact. One also observes that, after IR exposure, the nanoshells were often found to be nearby but detached from the damaged cells. This may be due to a change in the conformation of the epitope on the

cell surface that the antibody would normally attach to, or possibly to a lack of cell surface in general.

The presence of nanoshells with the *Escherichia coli* in the PBS buffer resulted in a measurable decrease in the population of viable *Escherichia coli*. This is believed to be due to random contact between the nanoshells that have been heated by the IR radiation and bacterial cells in the local vicinity. This incidental contact would be a non-specific form of nanoshell-bacterial cell interaction. Finally, the biofunctionalized nanoshells which had been decorated with antibodies specific for *Escherichia coli* were found to cause most of the cells to become non-viable. This result, combined with our observation of nanoshells binding to *Escherichia coli* bacterial cells, leads us to believe that the nanoshells are temporarily localized to the bacterial cells by the antibodies, and that this localization enhances the likelihood of a transfer of thermal energy from the nanoshell to the target species. This result is somewhat surprising when one considers the extremely small size of an antibody (a few nm) in comparison to both the nanoshell (a few hundred nm) and the *Escherichia coli* bacterial cell (a few thousand nm), as well as the type of interaction mechanism between the antibody and its epitope.

Dependence of *Escherichia coli* survivability on nanoshell concentration

Based on the results presented thus far, it is reasonable to conclude that the presence of biofunctionalized nanoshells in a solution with

Escherichia coli bacterial cells causes damage and/or death of at least some of the *Escherichia coli*. However, it is of interest to consider the dependence of lethality on the concentration of biofunctionalized nanoshells. A plot of the ratio dependence of viability of *Escherichia coli* with biofunctionalized nanoshells is shown in Figure 15. From the shape of this survival graph, we see a decrease in the survival rate of *Escherichia coli* as the ratio of the concentration of nanoshells to *Escherichia coli* CFUs increases. The center of the curve is ~3-4×10^4 NS/CFU, which suggests that there is a need for a few tens of thousands of nanoshells per *Escherichia coli* bacterial cell for a measurable drop in survival rate. However, when one considers the molar concentration of nanoshells in this solution (~10^{-18} M), it is still extremely small.

Figure 15. Nanoshell *Escherichia coli* survival graph.

Plot of ratio dependence of the survival of *Escherichia coli* with respect to the ratio of biofunctionalized nanoshells to CFUs. All experiments were performed in triplicate, and the error bars represent the standard deviation of the results from the mean.

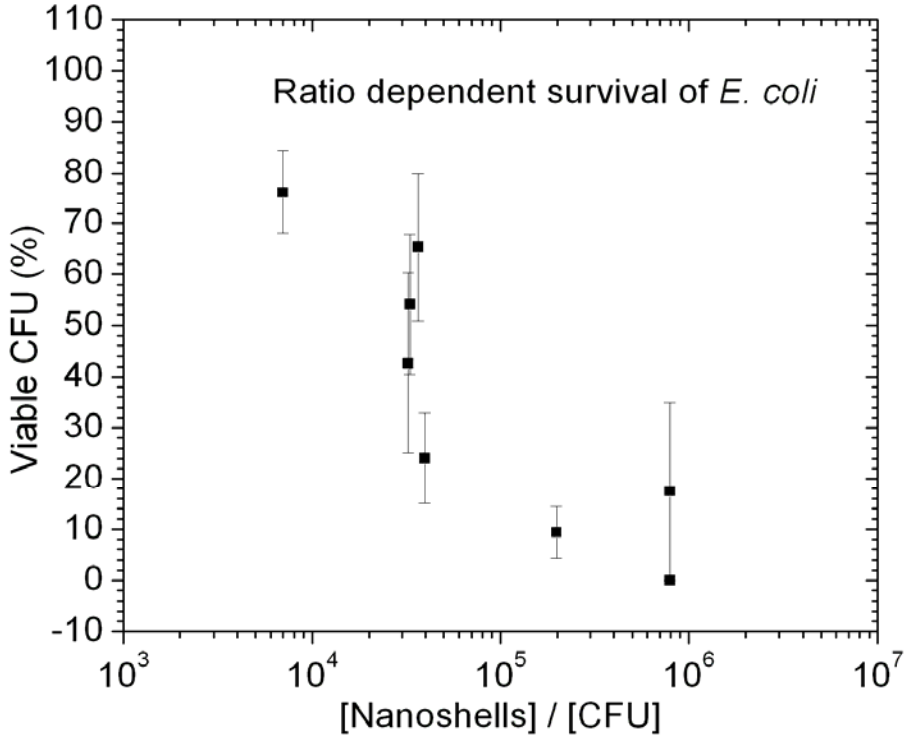
Ratio dependent survival of E. coli
Viable CFU (%)
110
100
90
80
70
60
50
40
30
20
10
0
-10
10^3
10^4
10^5
10^6
10^7
[Nanoshells] / [CFU]

Dependence of M13 bacteriophage survivability on nanoshell concentration

In addition to the *Escherichia coli* target described earlier, two other targets for damage by biofunctionalized nanoshells were explored in this research effort. The first is NS-73, which is an M13 bacteriophage specific for *Escherichia coli* that is obtained from a 7 mer library and shows an affinity for Au nanoshells as described in the Materials and Methods section of this thesis. The second is NS-32, which is also an M13 bacteriophage, but was panned from a 12 mer library. An image of NS-32 bacteriophage bound to nanoshells was shown in Figure 14. The NS-32 and NS-73 samples of M13 bacteriophage were each combined with nanoshells in different concentration ratios, and then exposed to the same 808 nm IR radiation conditions that were employed for the *Escherichia coli*. The results for the nanoshell to plaque forming units ratio dependence on the viability of phage is shown in Figure 16. As can be seen from the data in Figure 16, the shape of the curves are similar to that in Figure 15, but are shifted several orders of magnitude to the left. For NS-73, an approximately one-to-one ratio of nanoshells to bacteriophage results in a 50% reduction in plaque forming units. The NS-32 bacteriophage requires even fewer nanoshells for this same reduction. This difference in the required ratio of nanoshells to phage may be due to differences in the affinities of the two phage for the gold nanoshells. The reduced survival rate of NS-32 suggests the 12 mer library phage may have a slightly higher affinity for the gold nanoshells than NS-73,

a 7 mer library phage. The significantly lower survival rate we observe for nanoshells with respect to bacteriophage in comparison to the *Escherichia coli* is probably not due to a higher affinity of the bacteriophage for the gold nanoshell than that of the antibody for its epitope on the *Escherichia coli* bacterial cell. These are expected to be of a similar order of magnitude. Instead, one possibility is that it may be due to the gold nanoshell surface presenting a larger amount of “epitope” for the bacteriophage to bind to. Another possibility is that it may be due to statistical probability of encounter limitations. The probability that a nanoshell with antibodies on its surface will “find” an epitope on the surface of an *Escherichia coli* is expected to be smaller than the probability that a bacteriophage will find a nanoshell. The reduced survival rate may even be due to the bacteriophage being more susceptible to damage from the nanoshell that is the case for *Escherichia coli*.

Figure 16. M13 bacteriophage survival graph.

Plot of ratio dependence of survival of M13 bacteriophage on the ratio of nanoshells to PFUs. The bacteriophage controls were taken through all the same experimental procedure steps as the bacteriophage test samples, but were not exposed to IR radiation. All experiments were performed in triplicate, and the error bars represent the standard deviation of the results from the mean.

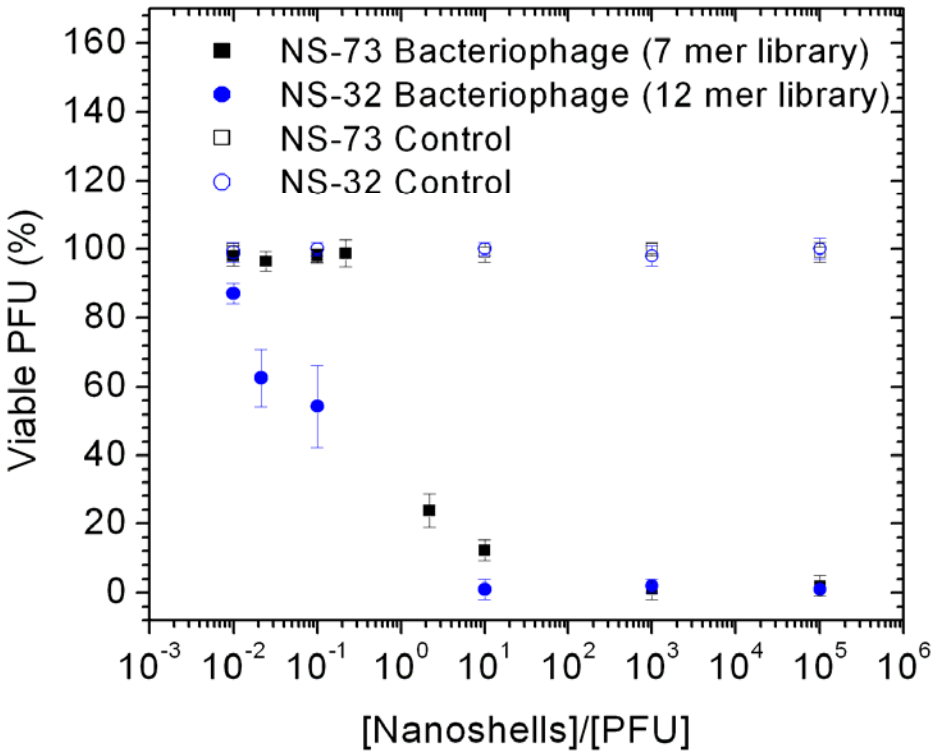
NS-73 Bacteriophage (7 mer library)
NS-32 Bacteriophage (12 mer library)
NS-73 Control
NS-32 Control
Viable PFU (%)
160
140
120
100
80
60
40
20
0
10^-3 10^-2 10^-1 10^0 10^1 10^2 10^3 10^4 10^5 10^6
[Nanoshells]/[PFU]

In summary, nanoshells with a desired absorption frequency in the IR wavelength range were utilized as a vehicle to receive energy from an IR laser source and transfer it to a target species. A protocol was developed for biofunctionalizing these nanoshells towards *Escherichia coli*. An apparatus was assembled that exposes the test subjects to 808 nm radiation at a controlled power level and time. It was demonstrated on the microscopic scale that the biofunctionalized nanoshells bind their target species, and that subsequent exposure to IR radiation causes damage to *Escherichia coli*. Further, the results were correlated to in vitro experiment with *Escherichia coli*. It was found that the presence of antibody-free nanoshells under IR irradiation causes what is believed to be nonspecific, collateral damage to *Escherichia coli* cells in the local area around the nanoshells. Also, a much greater decrease in the population of viable *Escherichia coli* was observed for the case of IR irradiation of nanoshells that have been biofunctionalized to specifically target *Escherichia coli*. This is believed to be due to the antibody temporarily localizing the biofunctionalized nanoshell to the target species, and therefore increasing the likelihood of thermal transfer from the nanoshell to the *Escherichia coli*. Finally, the viability of two different M13 bacteriophage that are specific for *Escherichia coli* and that have an affinity for gold nanoshells was explored as a function of nanoshell to bacteriophage concentration ratios. In this case, a significantly smaller concentration of nanoshells was required to achieve a 50% survival rate of plaque forming

units when exposed to the same IR radiation conditions as for the *Escherichia coli*.

Since attachment of biofunctionalized nanoshells has been observed to successfully target *Escherichia coli* as well as to interact with two different M13 bacteriophage, it is reasonable to conclude that this approach can be considered somewhat general in nature. The targeting of the biofunctionalized nanoshell depends only on the choice of biomolecular recognition motif for the desired target species. However, from a clinical standpoint, it is important to consider the concentration of nanoshells necessary for successfully combating the biological target. The high number of biofunctionalized nanoshells required under even ideal conditions to combat bacterial cells may preclude use of biofunctionalized nanoshells for this purpose from a clinical standpoint. However, smaller and less thermally stable biological targets such as bacteriophage or possibly DNA or other antibodies may be more amenable to regulation via biofunctionalized nanoshells. Based on the results of this research, no forgone conclusions can be drawn in regards to the effectiveness of biofunctionalized nanoshells in combating any particular biological target species. Instead, a detailed study will be necessary for each case considered.

APPENDIX A

SUPPLIMENTAL INFORMATION ON *Bacillus subtilis AS A TARGET SPECIES*

Attachment of biofunctionalized nanoshells to *Bacillus subtilis*

A scanning electron microscopy image of *Bacillus subtilis* spores incubated with nanoshell biofunctionalized with short peptides specific for the target species and a control peptide are shown in Figure 17. The nanoshells were in excess compared to the *Bacillus subtilis* spore concentration. Nanoshells are commonly seen bound to the *Bacillus subtilis* spores.

Effect of exposure to IR radiation on *Bacillus subtilis*

The effect of IR irradiation of *Bacillus subtilis* spores bound to nanoshells biofunctionalized with short peptides and exposed to 808 nm IR radiation is shown in Figure 18. The IR irradiation has clearly caused damage to the *Bacillus subtilis* spores. This can be seen by the change in the morphology of the bacterial spores, which appears to have lysed. Therefore, the laser radiation coupling to the biofunctionalized nanoshell has apparently

caused damage to the spore wall of the *Bacillus subtilis* spore to the point of lysing the cell. The nanoshell that was originally attached to the bacterial spore wall can still be seen near the top of the image.

Attachment of biofunctionalized nanoshells to *Bacillus subtilis*

The results for *Bacillus subtilis* spore bound to nanoshells biofunctionalized with short peptides and exposed to the same dose of 808 nm IR radiation that was shown in Figure 12 exhibited a similar level of damage to this significantly different target species as observed for the case of *Escherichia coli*. Such a result provides some encouragement that this technique is applicable to a broad range of biological targets.

Figure 17. Scanning electron microscopy image of *Bacillus subtilis* spore incubated with short peptide biofunctionalized nanoshells.

Scanning electron microscopy image of *Bacillus subtilis* bacterial spore incubated with short peptide biofunctionalized nanoshells. (A) Individual *Bacillus subtilis* bacterial spore with biofunctionalized nanoshells in higher resolution image (arrow points to nanoshell). (B) Four panel collage of scanning electron microscopy images showing nanoshells biofunctionalized with short peptides that are bound to *Bacillus subtilis* spores (panels a-c), as well as a control sample (panel d) utilizing nanoshells biofunctionalized with the Flg-A3C peptide which is not specific for *Bacillus subtilis*. The scale bars shown in each panel are 500 nm in length.

Figure 17 A

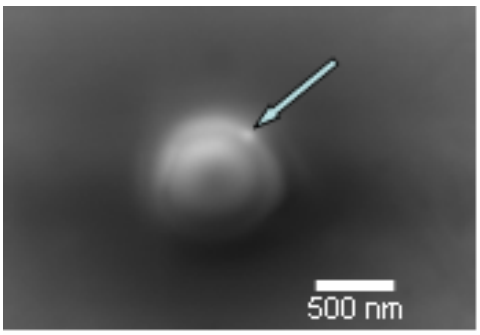

Figure 17 B

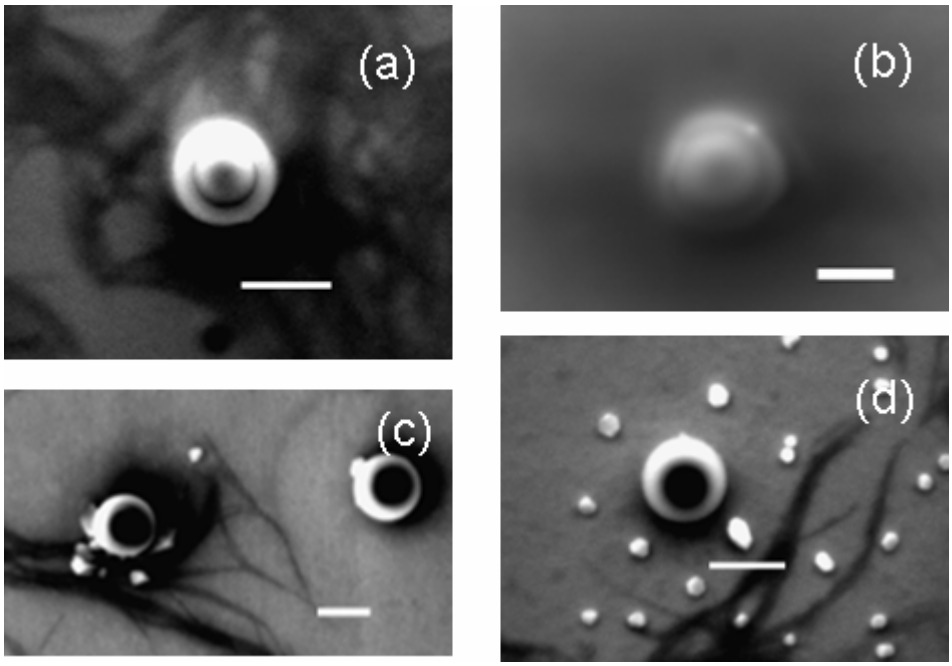

Figure 18. Scanning electron microscopy image of *Bacillus subtilis* spores incubated with short peptide biofunctionalized nanoshells and exposed to 808 nm laser radiation.

Scanning electron microscopy image of *Bacillus subtilis* spore bound to short peptide biofunctionalized nanoshell and exposed to 808 nm radiation for 5 minutes at 1 W cm^{-2}. The nanoshell location is indicated by the arrow. (A) Individual *Bacillus subtilis* with nanoshells exposed to IR radiation in higher resolution image. (B) Six panel collage of images showing different *Bacillus subtilis* that were bound to nanoshells and exposed to IR radiation. The scale bars shown in each panel are 500 nm in length.

Figure 18 A

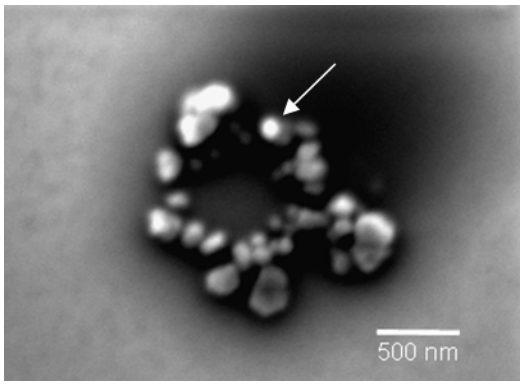

Figure 18 B

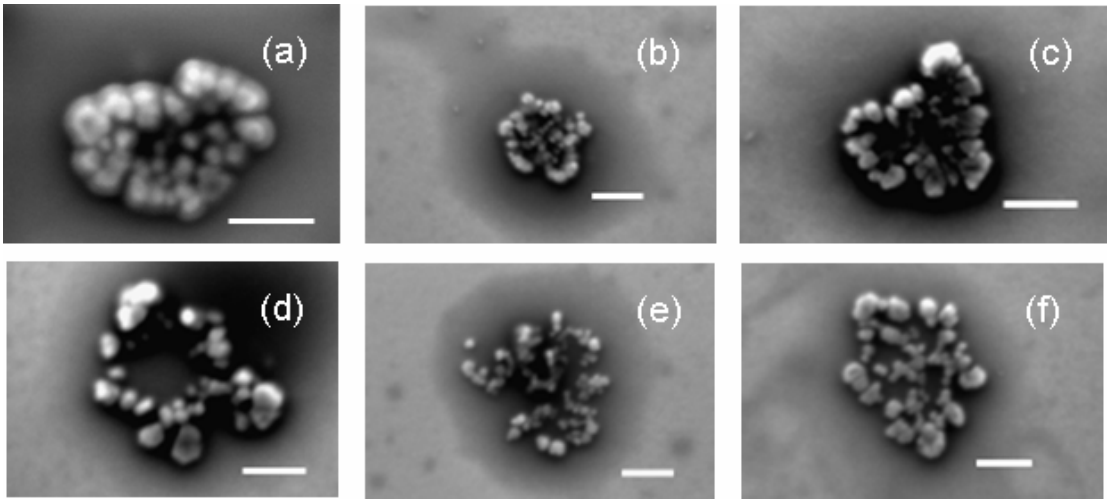

BIBLIOGRAPHY

Atlas, R.M. (2001). Bioterrorism before and after September 11. Crit. Rev. Microbiol. *27*, 355-379.

Atlas, R.M. (2002). Bioterrorism: From threat to reality. Annu. Rev. Microbiol. *56*, 167-185.

Bell, C.A. and Uhl, R.J. (2002). Detection of *Bacillus anthracis* DNA by LightCycler PCR. J. Clin. Microbiol. *40*, 2897-2902.

Bertin, P.A., Gibbs, J.M., Shen, C.K-F., Thaxton, C.S., Russin, W.A., Mirkin, C.A., and Nguyen, S.T. (2006). Multifunctional polymeric nanoparticles from diverse bioactive agents. J. Am. Chem. Soc. *128*, 4168-4169.

Bhalla, D.K. and Warheit, D.B. (2004). Biological agents with potential for misuse: a historical perspective and defensive measures. Toxicol. Appl. Pharmacol. *199*, 71-84.

Cuenca, A.G., Jiang, H., Hochwald, S.N., Delano, M., Cance, W.G., and Grobmyer, S.R. (2006). Emerging implications of nanotechnology on cancer diagnostics and therapeutics. CANCER *107*, 459-466.

Dhayal, B., Henne, W.A., Doorneweerd, D.D., Reifenberger, R.G., and Low, P.S. (2006). Detection of *Bacillus subtilis* spores using peptide-functionalized cantilever arrays. J. Am. Chem. Soc. *128*, 3716-3721.

Dillenback, L.M., Goodrich, G.P., and Keating, C.D. (2005). Temperature-programmed assembly of DNA:Au nanoparticle bioconjugates. Nano Lett. *6*, 16-23.

Duff, D.G. and Baiker, A. (1993). A new hydrosol of gold clusters. 1. Formation and particle size variation. Langmuir *9* 2301-2309.

Hirsch, L.R., Jackson, J.B., Lee, A., Halas, N.J., and West, J.L. (2003). A whole blood immunoassay using gold nanoshells. Anal. Chem. *75*, 2377-2381.

Hirsch, L.R., Stafford, R.J., Bankson, J.A., Sershen, S.R., Rivera, B., Price, R.E., Hazle, J.D., Halas, N.J., and West, J.L. (2003). Proc. Natl. Acad. Sci. *100*, 13549-13554.

Jackson, J.B, Westcott, S.L., Hirsch, L.R., West, J.L., and Halas, N.J. (2003). Controlling the surface enhanced Raman effect via the nanoshell geometry. Appl. Phys. Lett. *82*, 257-259.

Jiang, X., Shang, L., Wang, Y., and Dong, S. (2005). Cytochrome *c* superstructure biocomposite nucleated by gold nanoparticle: thermal stability and voltammetric behavior. Biomacromolecules *6*, 3030-3036.

Kalele, S.A., Kundu, A.A., Gosavi, S.W., Deobagkar, D.N., Deobagkar, D.D., and Kulkarni, S.K. (2006). Rapid detection of *Escherichia coli* by using antibody-conjugated silver nanoshells. Small *2*, 335-338.

Knurr, J., Benedek, O., Heslop, J., Vinson, R.B., Boydston, J.A., McAndrew, J., Kearney, J.F., and Turnbough, C.L., Jr. (2003). Peptide ligands that bind selectively to spores of *Bacillus subtilis* and closely related species. Appl. Environ. Microbiol. *69*, 6841-6847.

Lin, A.W.H., Lewinski, N.A., West, J.L., Halas, N.J., and Drezek, R.A. (2005). Optically tunable nanoparticle contrast agents for early cancer detection: model-based analysis of gold nanoshells. J. Biomed. Optics *10*, 064035-1-10.

Lin, A.W.H., Loo, C.H., Hirsch, L.R., Barton, J.K., Lee, M.-H., Halas, N.J., West, J.L., and Drezek, R.A. (2004). Nanoshells for integrated diagnosis and therapy of cancer. Proc. SPIE *5593*, 308-316.

Loo, C., Lowery, A., Halas, N., West, J., and Drezek, R. (2005). Immunotargeted nanoshells for integrated cancer imaging and therapy. Nano Letters *5*, 709-711.

Mortensen, M.W., Björkdahl, O., Sørensen, P.G., Hansen, T., Jensen, M.R., Gundersen, H.J.G., and Bjornholm, T. (2006). Functionalization and cellular uptake of boron carbide nanoparticles. The first step toward T cell-guided Boron neutron capture therapy. Bioconjugate Chem. *17*, 284-290.

New England BioLabs, (2002). Ph.D. Phage Display Peptide Library Kit – Instruction Manual. Cat. #E8110S, Ver. 2.7.

Oldenburg, S.J., J.B. Jackson, Westcott, S.L., and Halas, N.J. (1999). Infrared extinction properties of gold nanoshells. Appl. Phys. Lett. *75*, 2897-2899.

O'Neal, D.P., Hirsch, L.R., Halas, N.J., Payne, J.D., and West, J.L. (2005). Photo-thermal cancer therapy using intravenously injected near infrared-absorbing nanoparticles. Proc. SPIE *5689*, 149-157.

Prodan, E., Nordlander, P., and Halas, N.J., (2003). Electronic structure and optical properties of gold nanoshells. Nano Lett. *3*, 1411-1415.

Rozenzhak, S.M., Kadakia, M.P., Caserta, T.M., Westbrook, T.R., Stone, M.O., and Naik, R.R. (2005). Cellular internalization and targeting of semiconductor quantum dots. Chem. Commun. 2217-2219.

Slocik, J.M., Tam, F., Halas, N.J., and Naik, R.R. (2007). Peptide-assembled optically responsive nanoparticle complexes. Nano Lett., *7*, 1054-1058.

Souza, G.R., Christianson, D.R., Staquicini, F.I., Ozawa, M.G., Snyder, E.Y., Sidman, R.L., Miller, J.H., Arap, W., and Pasqualini, R. (2006). Networks of gold nanoparticles and bacteriophage as biological sensors and cell-targeting agents. Proc. Nat. Aca. Sci. *103*, 1215-1220.

Stöber, W. and Fink, A. (1968). Controlled growth of monodisperse silica spheres in the micron size range. J. Colloid. Interface Sci., *26*, 62-69.

Wang, H., Levin, C.S., and Halas, N.J. (2005). Nanosphere arrays with controlled sub-10-nm gaps as surface-enhanced Raman spectroscopy substrates. J. Am. Chem. Soc. *127*, 14992-14993.

You, C.-C., De, M., Han, G., and Rotello, V.M. (2005). Tunable inhibition and denaturation of α-chymotrypsin with amino acid-functionalized gold nanoparticles.

Zhang, J. and Ji, H.-F. (2004). An anti *E. coli* O157:H7 antibody-immobilized microcantilever for the detection of *Escherichia coli* (*E. coli*). Anal. Sci. *20*, 585-587.